Heliyon 10 (2024) e37247

Contents lists available at ScienceDirect

Heliyon

journal homepage: www.cell.com/heliyon

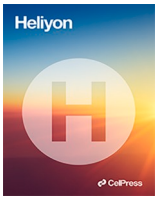

Research article

Evolution characteristics and driving factors of potential non-point source pollution risks in a watershed affected by land use changes

Xiaolan Meng [a,*], Fujun Xu [a], Yuanjia Huang [b,c,d], Xing Zhang [a], Mantong Zhang [a]

[a] Xi 'an Academy of Environmental Protection Science, Xi'an 710061, China
[b] School of Water and Environment, Chang'an University, Xi'an 710054, China
[c] Key Laboratory of Subsurface Hydrology and Ecological Effect in Arid Region of the Ministry of Education, Chang'an University, Xi'an 710054, China
[d] Key Laboratory of Eco-hydrology and Water Security in Arid and Semi-arid Regions of Ministry of Water Resources, Chang'an University, Xi'an 710054, China

ARTICLE INFO

Keywords:
Land use changes
Non-point source pollution (NPS)
Potential non-point pollution index (PNPI)
Risk management
Spatiotemporal change characteristics
Heihe watershed
Qinling mountains

ABSTRACT

Land use types, land development and utilization intensity within watersheds have changed based on intensifying human activities and climate change, thereby inducing spatiotemporal variations in non-point source pollution (NPS), significantly impacting soil and water quality. This study performed a case study on an ecological environment functional zone at the northern foot of Qinling Mountains, an area strongly affected by human activities and land use changes. It employed an improved potential non-point pollution index (PNPI) model to analyze potential non-point source pollution (PNPS) and associated risk evolution characteristics in watershed over the past 30 years. The results indicate that from 1990 to 2020, the dominant land use categories were forest and arable land, making up 95 % of the entire watershed area. Notably, urban residential land presented the most significant expansion rates and nearly doubled in area between 1990 and 2020, whereas shrubland, grassland, and unused land showed a decreasing trend. With the application of the quantile classification method, PNPS risk values were divided into five categories: very low, low, moderate, high, and very high. A polarized trend in risk was observed, with increases in areas influenced by human activities and rapid expansion of very high-risk regions. Concurrently, the pollution risk in the upstream water source area decreased. In recent years, accelerated urbanization has been the main driver causing expansion of high PNPS risk regions. This study explores the spatial and temporal evolution of PNPS risk in the Heihe Basin by using an improved PNPI model. The improved model is more accurate in calculations and provides a better understanding of the distribution of PNPS, which is an important reference for watershed management and water resource governance.

1. Research background

Northern China is currently experiencing a natural shortage of water resources, and the quality of surface water and groundwater in watersheds is being increasingly threatened by climate change and large-scale urbanization. Currently, the scarcity of water resources and water pollution have become severe challenges for achieving economic and social sustainable development to build a 'Beautiful

* Corresponding author.
E-mail address: 13359243070@163.com (X. Meng).

https://doi.org/10.1016/j.heliyon.2024.e37247
Received 14 June 2024; Received in revised form 12 August 2024; Accepted 29 August 2024
Available online 30 August 2024

China' [1]. Watershed pollution sources generally include point and non-point sources. Due to fixed pollution source origins and easy-to-implement monitoring methods, point source water pollution in watersheds has been effectively controlled in recent years through the joint efforts of the government at various levels and research institutions. In contrast, non-point source pollution (NPS) in watersheds is widespread and decentralized, making it more complex to identify, control, and govern. As a result, NPS has become a bottleneck in improving the water environment quality of watersheds [2,3]. NPS mainly originates from various pollutants present in run-off generated from farmland, urban areas, and other sources [4,5]. Effective management measures are essential for controlling non-point sources. It has been demonstrated that initiatives such as land use planning, sustainable agriculture and optimal land management are effective in reducing the impact of NPS in watersheds [5–7]. The most significant factor influencing changes in NPS is land use change. Consequently, research on the relationship between land use change and NPS is becoming increasingly pertinent [8–10].

Quantifying NPS is essential for effectively controlling this type of pollution in watersheds. Significant advances have been made in recent years in the analysis and modelling of NPS, employing remote sensing, catchment modelling and field sampling [11–18]. However, accurately quantifying the sources and effects of NPS remains highly challenging [19]. Currently, most non-point source quantification methods are model-based, with the Soil & Water Assessment Tool (SWAT), Answers Areal Nonpoint Source Watershed Environment Response Simulation (ANSWERS), Annualized Agricultural Non-Point Source Pollution Model (AnnAGNPS) representing the most popular methods. While these models can accurately simulate the environmental responses in watersheds to NPS, they have high requirements in terms of data volume and data precision; moreover, they are not appropriate for watersheds lacking monitoring data [20–23]. The potential non-point pollution index (PNPI) model, a Geographic Information System (GIS)-based tool for assessing the risk of NPS in watersheds, has garnered increasing research interest due to its minimal data requirements and high accuracy [24,25]. The Potential Non-Point Pollution Index (PNPI) model integrates hydrological, geological, and land use factors that contribute to non-point source pollution. It quantitatively characterizes potential regional non-point source (NPS) risks by generalizing the production, degradation, and transportation processes of pollutants [11,16,26–29]. Researchers have employed the PNPI model to assess the distribution of potential non-point pollution risk in various regions, including the Province of Viterbo in central Italy [30] and typical watersheds in China [18,19,31–35]. Currently, most research on the PNPI and its enhanced models focuses on evaluating NPS risks in small watersheds. However, there is a scarcity of studies examining the impact of historical land use changes on the evolution of NPS risks and strategies for mitigating these risks in watersheds [29,36,37]. In summary, the PNPI model serves as a valuable tool for simulating and managing non-point source pollution in watersheds. By considering a broad range of factors, the PNPI model offers a comprehensive understanding of the potential for non-point source pollution and can inform effective pollution control measures.

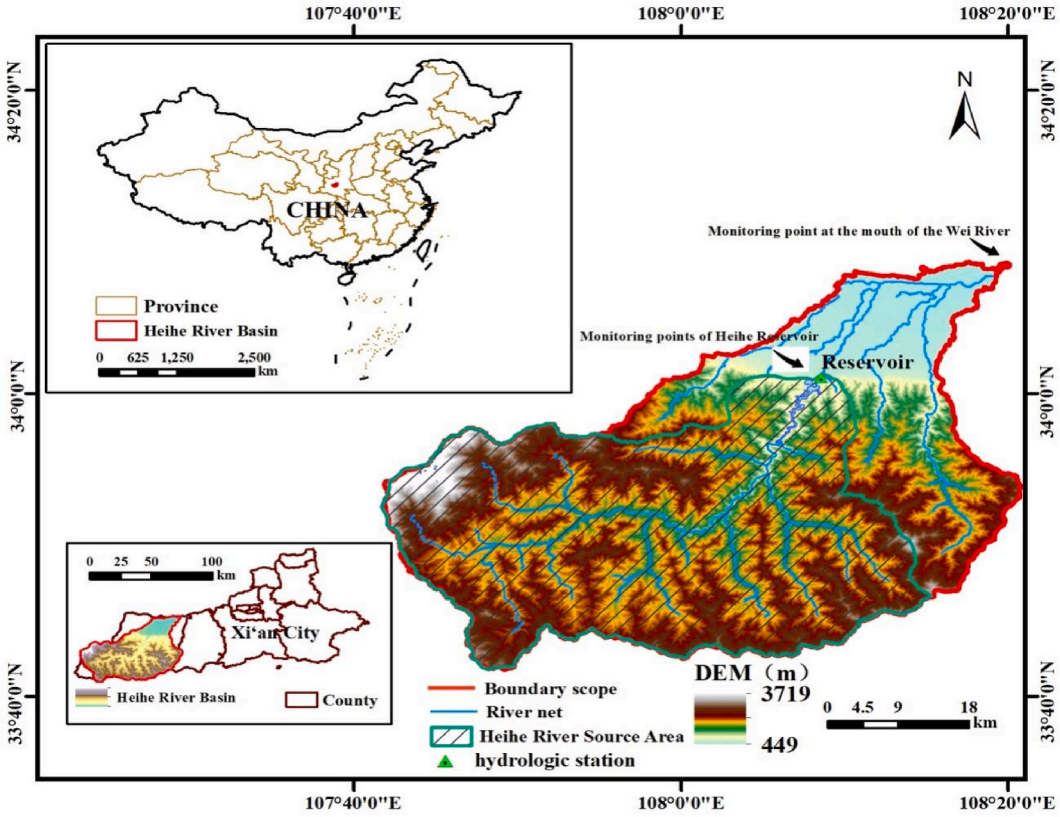

Fig. 1. Location of the study area.

The Qinling Mountains, spanning Shaanxi, Gansu, and Henan provinces, are the climatic boundary between northern and southern China and the associated watershed extends between the Yellow and Yangtze rivers. These mountains serve as a geographical landmark and ecological security barrier for China and have multiple functions, such as climate regulation, soil and water conservation, water source conservation, and biodiversity maintenance [38,39]. The mountainous area at the northern foot of the Qinling Mountains lies between the mountains' drainage divide and southern edge of the Guanzhong Plain, and serves as an important water conservation area and drinking water source for the plain with important ecological and environmental functions. Compared to the Guanzhong Plain, the mountainous area has relatively abundant water resources and good water quality, thus providing significant water resource support for the sustainable socio-economic development on the plain. However, the socio-economic development of the Guanzhong Plain, especially in Xi'an City, has occurred at a rapid pace, with accelerated urbanization. Against this backdrop, water consumption for industry, agriculture, daily life, and ecology has sharply increased. As a result, ecological and environmental issues such as river pollution and vegetation destruction have become increasingly prominent and water environment pollution is intensifying. Watershed water resource protection is a crucial task for ecological conservation in the Qinling Mountain region and represents a core as well as key issue for the sustainable socio-economic development of the Guanzhong Plain. Xi'an City, as the central city of the Guanzhong Plain, has a per capita water availability of 187 m^3, which is only 1/6th and 1/8th of the provincial and national averages, respectively, making it a typical resource-deficient city. The Heihe Jinpen Reservoir in the upper reaches of the Heihe watershed is the largest drinking water source of Xi'an City (location Fig. 1) and provides approximately 380 million m^3 of drinking water to the city annually, accounting for over 76 % of the city's total water supply. Therefore, the Heihe River has hailed as the "Mother River" of the people of Xi'an. In recent years, point source pollution in the Heihe watershed is being effectively controlled, leading to a significant improvement in water quality. However, the concentrations of nutrients such as nitrogen and phosphorus in the water have been increasing year on year. The nitrogen and phosphorus indicators in the watershed are mainly attributed to NPS. Therefore, it is imperative to study the PNPS risks within the watershed [40–43]. In this study, the Heihe watershed in Xi'an City, situated at the northern foot of the Qinling Mountains, was selected as the research site. Based on the improved PNPI model, the spatiotemporal evolution characteristics of PNPS risks influenced by land use changes in the Heihe watershed from 1990 to 2020 were explored to identify the dominant driving factors. The findings of this study offer a foundational reference for managing water resources and governing the water environment within the watershed.

2. Overview of the study area

The Heihe watershed is situated in the mountainous area at the northern foot of the Qinling Mountains. Its geographic coordinates range from 107°43′ E to 108°24′E and 33°42′ N to 34°13′N. Originating at the main peak of Mount Taibai in the Qinling Mountains, the Heihe River is a major tributary of the Weihe River system within the Yellow River watershed. It flows from southwest to northeast and enters the Weihe River at Shima Village, Shangcun Town, Zhouzhi County, Xi'an City, Shaanxi Province. The total length of the main stream is 125.8 km, with a watershed area of 2258 km^2. According to data measured at the Heiyukou hydrological station within the watershed (located at 108.210°E, 34.058°N in Wujia Village, Mazhao Town, Zhouzhi County) from 1956 to 2005, the average annual precipitation and run-off in the region are 635.2 mm and 545.22 million m^3, respectively. The maximum and minimum annual precipitation are 1180.9 mm and 526.2 mm, respectively, which are 1.4 and 0.62 times the average value, respectively. Precipitation is mainly concentrated from July to October, comprising 59.5 % of the annual total. In contrast, the dry season from November to March contributes about 10 % of the annual precipitation.

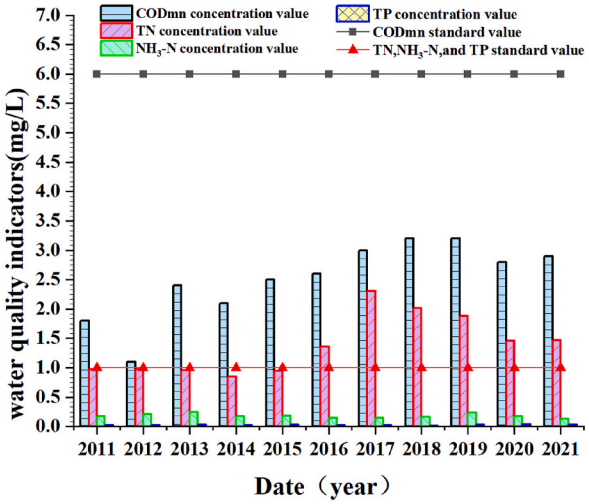

Fig. 2. Changes in monitored indicator values of Heihe Reservoir water source area from 2011 to 2021. Changes in the a) chemical oxygen demand based on the potassium permanganate index; b) total nitrogen and ammonia nitrogen concentrations, and c) total phosphorus concentrations in the water source area from 2011 to 2021.

Long-term agricultural activities in the middle and lower reaches of the Heihe River have consistently exerted significant pressure on the regional water environment. In recent years, the expansion of construction land in the region has also had a considerable impact on the watershed's water environment. Detailed watershed location information has been shown in Fig. 1. Along the Heihe River, two water quality monitoring sections were set up: one at the Heihe Reservoir and the other at the confluence of the Heihe and Weihe rivers. Based on water quality monitoring data from 2001 to 2020, the water quality at the confluence of the rivers was inferior and ranged from Class V to Class IV from 2001 to 2014 but improved to Class III and to Class II from 2015 to 2020. The water quality at the Heihe Reservoir water source monitoring point ranged from Class III to Class II between 2011 and 2021. According to the water quality conditions, four nutrient indicators, i.e., permanganate index, total nitrogen, ammonia nitrogen, and total phosphorus, were selected for analysis, as shown in Fig. 2. The results indicate that total nitrogen was the main indicator exceeding Class II water quality standards, total phosphorus shows a relatively stable trend, while the permanganate index and ammonia nitrogen indicator exhibit increasing trend [41–43]. The Heihe watershed is a forest ecosystem dominated by warm and humid, deciduous broad-leaved forests. Its vegetation can be divided (from top to bottom) into three zones: deciduous broad-leaved forest, coniferous forest, and shrub meadow. Forest coverage is above 90 % in the water source area in the upper section of the Heihe River.

3. Research Content and methods

3.1. Improvement of the PNPI model utilizing the coefficient of variation decision method

Due to the convenient accessibility of data, the PNPI model has become a principal approach for gauging the potential risk of PNPS for diverse land uses within a watershed [11,24,31]. This model conceptualizes the generation, degradation, and transport processes of pollutants into spatially distributed land cover indicators, distance indicators, and run-off indicators. The spatial PNPS risks of the watershed are subsequently represented as a function of these three indicators [32]. The PNPI model combines the functions of the three indicators based on fixed weights determined by expert scoring, which compromises the objectivity and applicability of the model. To overcome the limitations in objectivity and applicability inherent in the PNPI model, this study employed an objective weighting approach grounded in the principle of information entropy. Specifically, the coefficient of variation decision method was used to enhance the robustness and accuracy of the model [18,33]. The structure of this improved model has been illustrated in Fig. 3.

The improved PNPI model calculates the spatial and temporal dynamics of PNPS in the watershed, reflecting the impact of land use changes over the past 30 years. Combined with spatial and temporal land-use change characteristics, this approach reveals the main

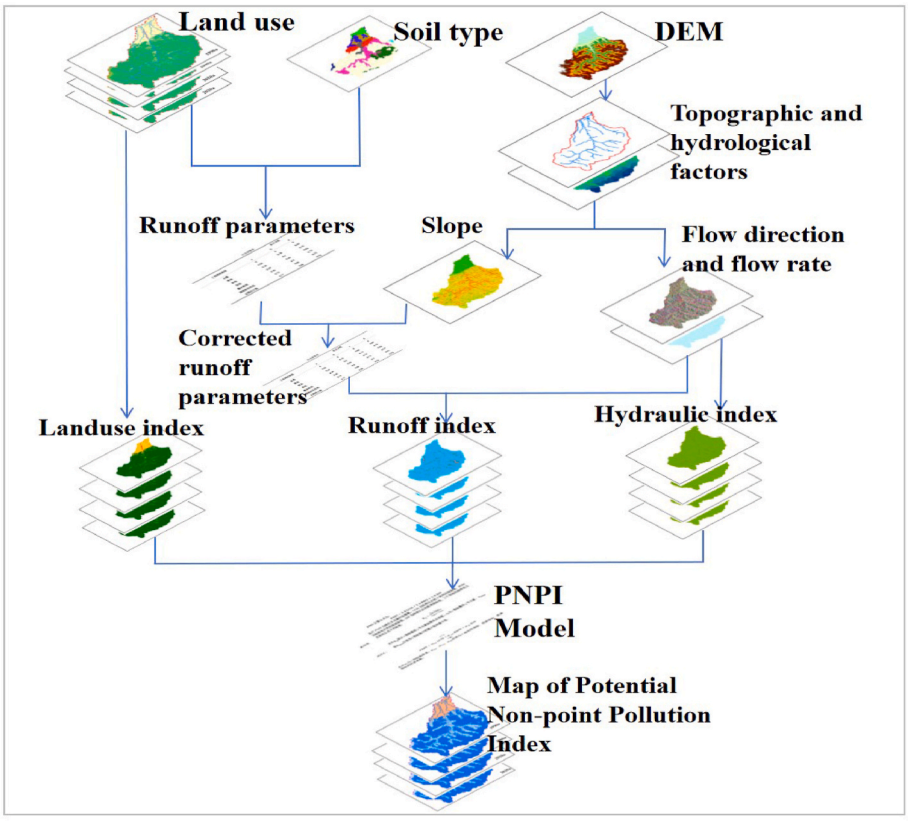

Fig. 3. Structure of the improved PNPI model.

distribution and evolution characteristics of pollution risks and their driving factors.

3.2. Data sources and data processing

The data required for the PNPI model calculations mainly consist of spatial and attribute data. Spatial data includes digital elevation map (DEM), soil type map, and land use map, while attribute data comprise soil permeability data and land use attribute data. The sources of the data required for model calculations have been listed in Table 1. Soil permeability was classified based on the Harmonized World Soil Database (HWSD). Using SPAW (Soil-Plant-Air-Water) 6.02 software developed by the U.S. Department of Agriculture, the saturated infiltration rates of various soils were calculated, and then the permeability was classified into four groups (A, B, C, and D) based on the Hydrologic Soil Groups (HYDGRP) standards of the U.S. Natural Resources Conservation Service (NRCS). Class B and C were the main hydrological soil groups in the study area. Land use attribute data included indicator values of various land uses and run-off parameters under different hydrologic soil groups, which were both obtained from existing expert scoring and parameter systems of the PNPI or extrapolated based on field experiments.

Due to differences in the calibration and acquisition of spatial data sources as well as the coordinate systems used for the source data, the data was pre-processed and standardized into a consistent projection coordinate system suitable for the study area to facilitate subsequent calculations. Depending on the study area's size, data acquisition situation, and research accuracy requirements, the grid data were consistently resampled into 30 m × 30 m. The soil types in the study area and the representative annual land use types selected have been shown in Figs. 4 and 5, respectively.

3.3. Land cover indicator

The Land Cover Indicator (LCI) assesses the potential pollution discharged from different land use types and its impact on the aquatic environment when it enters water bodies. The higher the land cover indicator for a particular land use type, the greater its potential pollutant load, indicating a higher pollution risk. Drawing on existing research findings [11], the LCI of the PNPI model was determined through expert scoring. Using their professional expertise, experts assessed the potential pollutant yield of various land use types, assigning scores on a scale from 0 to 10. When more experts were involved in the scoring, the covered research fields were broader, and the standard deviation of the scores were lower, with results being more reliable. Land use types in the study area were selected from Cecchi et al. [11,25], and the land cover indicator values and standard deviation of the scores were then determined (Table 2).

3.4. Distance indicator and run-off indicator

The Distance Indicator (DI) generalizes the degradation processes of pollutants throughout their migration path to the confluence [24]. A higher distance indicator corresponds to a shorter distance to the river and a lower impact of the pollutant degradation process, thereby resulting in an increased pollution risk. The distance indicator was calculated as follows Eq. (1):

$$DI = Exp(-(D \cdot k)) \tag{1}$$

where DI is the distance indicator value; D is the length of the confluence expressed as the number of cell grids; and k is a constant. k was set to 0.090533 based on research by Cecchi et al. [18,24,44,45].

The Run-off Indicator (ROI) generalizes the transport, infiltration, and filtration processes of pollutants, which are influenced by terrain, soil, and land use factors. ROI is inversely related to infiltration and filtration strength, with higher indicators resulting in more pollutants flowing into the water bodies, thereby escalating the pollution risk. The run-off indicator was calculated as follows Eqs. (2) and (3):

Table 1
Data requirements for the PNPI model and data sources for this study.

Type	Name	Data format	Data overview	Data name	Source
Spatial data	Digital elevation map	Grid	12.5 m × 12.5 m resolution	AW3D30	Japan Aerospace Exploration Agency (JAXA) (https://nasadaacs.eos.nasa.gov/)
	Soil type map	Grid	500 m × 500 m resolution	HWSD	National Cryosphere Desert Data Center (www.ncdc.ac.cn)
	Land use map	Grid	30 m × 30 m resolution	CLCD	Institute of Remote Sensing Information Processing, Wuhan University (http://irsip.whu.edu.cn/)
Attribute data	Soil permeability data	csv	Soil permeability levels within the study area	–	Calculated based on HWSD soil parameters or using SPAW
	Land use attribute data	csv	Empirical parameters of various land use types within the study area	–	Compared with the European CORINE land use classification to obtain empirical coefficients from the PNPI model

Note: HWSD, Harmonized World Soil Database; SPAW, Soil-Plant-Air-Water; CORINE, Coordination of Information on the Environment; CLCD, China land cover dataset; PNPI, potential non-point pollution index.

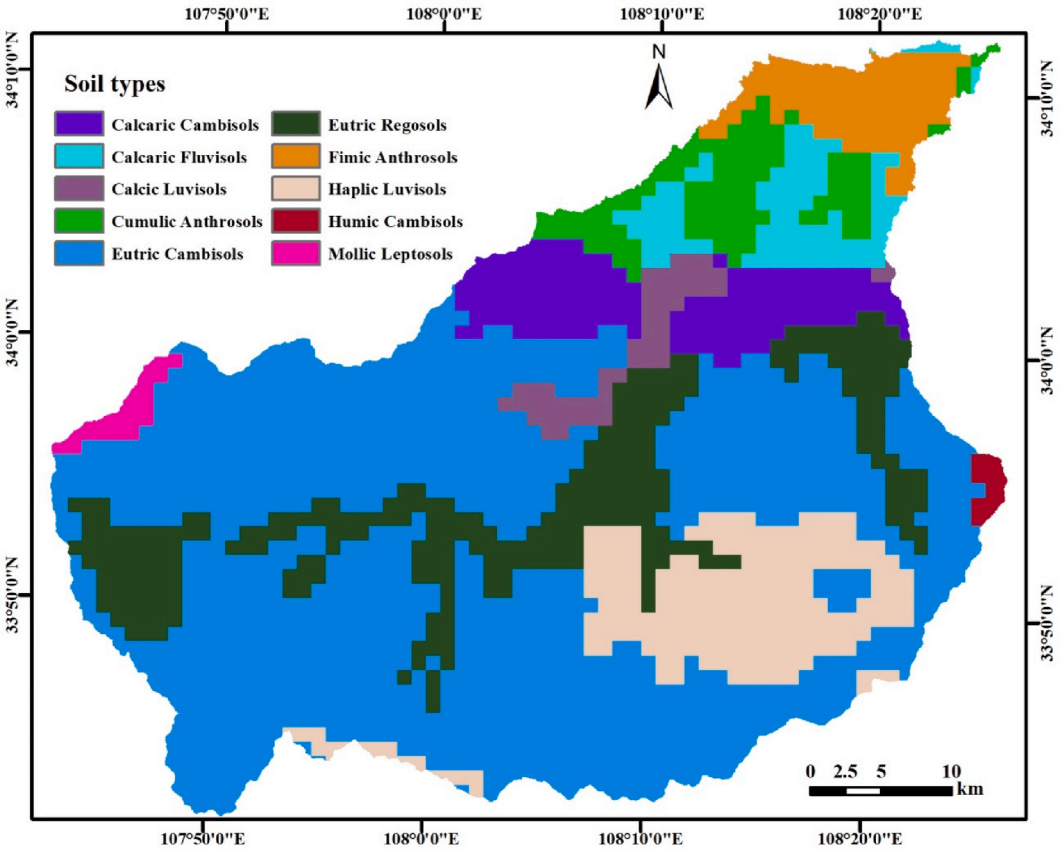

Fig. 4. Soil type map.

$$ROI = \left(\sum_{i=1}^{n} CROP_i \right) \Big/ n \tag{2}$$

$$CROP = ROP + C \tag{3}$$

where *ROI* is the run-off indicator value; $CROP_i$ is the run-off parameter for the *i*th unit slope on the confluence path, ranging from 0 to 1 (When the result of Eq. (3) is greater than 1, the result is 1); *n* is the number of units on the confluence path; and *ROP* is the run-off parameter. Table of run-off coefficient for different land use types and hydrological soil groups and slope correction coefficients C in the study area, as presented in Checchi et al. [18,24,44,45] (Table 3).

3.5. Potential non-point pollution index

The PNPI provides a generalized assessment of the pollutant load intensity exerted by different land use activities impacting rivers and other surface water systems throughout a watershed, and it integrates land cover indicators, distance indicators, and run-off indicators. The original PNPI model is calculated via expert scoring [11,24] using fixed weights, which leads to shortcomings in objectivity and practicality. The PNPI was calculated as follows Eq. (4):

$$PNPI = 4.8 \cdot LCIS + 2.6 \cdot ROIS + 2.6 \cdot DIS \tag{4}$$

where *PNPI* is the potential non-point index; *LCIS* is the standardized land cover indicator value; *ROIS* is the standardized run-off indicator value; and *DIS* is the standardized distance indicator value. The three indicators are standardized by Eq. (5):

$$X_{ij} = \frac{x_{ij} - x_{imin}}{x_{imax} - x_{imin}} \tag{5}$$

where X_{ij} is the standardized value of the *j*th element in the *i*th indicator set; x_{ij} is the *j*th element of the *i*th indicator set; and x_{imax} and x_{imin} are the maximum and minimum values in the *i*th indicator set, respectively.

The coefficient of variation decision method assigns weights to variables based on the relative change in amplitude of each in-

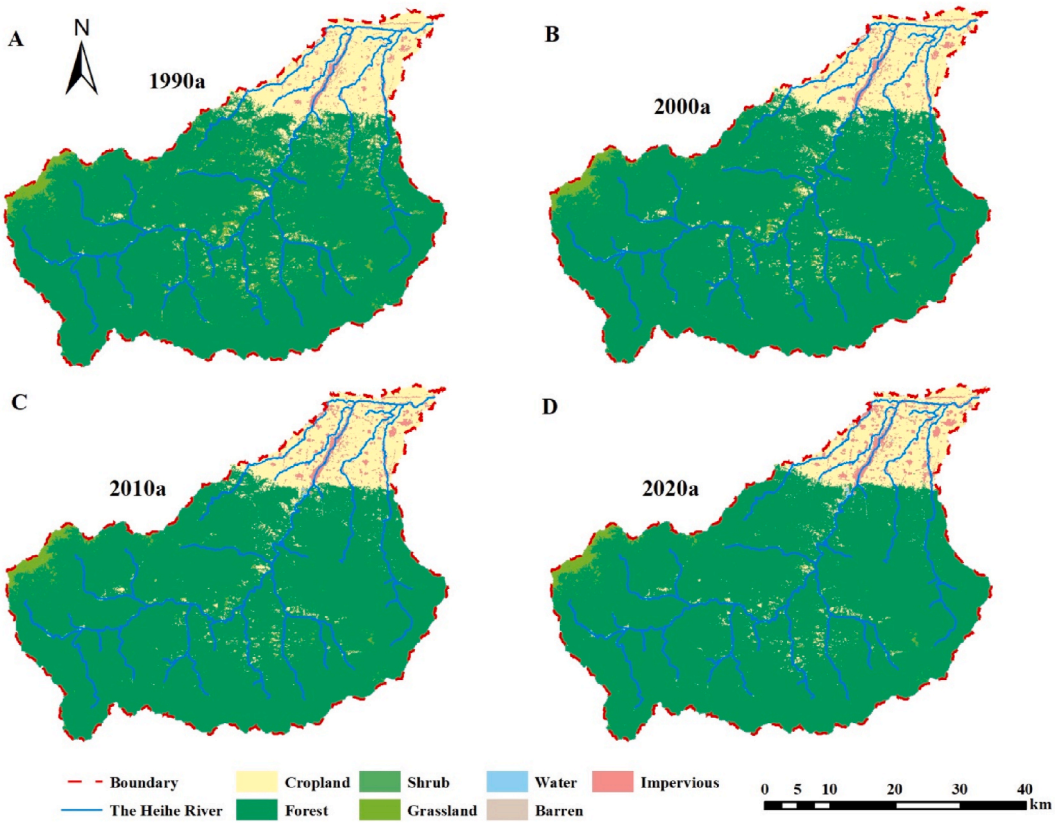

Fig. 5. Representative annual land use map.

Table 2
Land cover indicators.

Type of land use	Land use indicator (0–10)	Standard deviation
Water bodies	0.14	0.38
Arable land	7.73	2.16
Forest land	0.44	0.88
Grassland	1.94	2.27
Shrubland	0.78	1.09
Urban residential land	8.22	2.22
Unused land	0	0

Table 3
Run-off coefficient table.

Type of land use	Hydrologic soil group			
	a	b	c	d
Water bodies	0	0	0	0
Arable land	0.66	0.78	0.85	0.89
Forest land	0.36	0.6	0.73	0.79
Grassland	0.49	0.69	0.79	0.84
Shrubland	0.36	0.6	0.73	0.79
Urban residential land	0.75	0.85	0.9	0.92
Unused land	0.77	0.86	0.91	0.94

dicator, and it is free from subjective factors and capable of yielding more rigorous weight coefficients [24]. This method was used to optimize the weights used in the original model while integrating the three indicators. The detailed calculation steps are as follows.

1) Calculate the coefficient of variation for each indicator, see Eq. (6):

$$C.V._{\cdot i} = \frac{\sigma_i}{\overline{X_i}} \tag{6}$$

where, $C.V._{\cdot i}$, $\overline{X_i}$ and σ_i are the coefficient of variation, mean, and standard deviation of the ith indicator set, respectively.

2) Calculate the weights for each indicator and obtain the PNPI value, see Eqs. (7) and (8):

$$w_i = \frac{C.V._{\cdot i}}{\sum_{i=1}^{m} C.V._{\cdot i}} \tag{7}$$

$$PNPI = w_{lci} \cdot LCIS + w_{roi} \cdot ROIS + w_{di} \cdot DIS \tag{8}$$

where w_i is the weight of the ith indicator set; and w_{lci}, w_{roi}, and w_{di} are the weight coefficients of the land cover, run-off, and distance indicators, respectively.

4. Results and analysis

4.1. Spatiotemporal analysis of land use changes

The land use conditions for representative years within the study area were statistically analyzed to obtain a land cover map (Fig. 6). In the watershed, forest land and arable land were the dominant land use types, consistently comprising around 95 % of the total area. Between 1990 and 2020, the land use types that decreased in area included shrubland, grassland, and unused land. Among them, grassland and shrubland shrank at the fastest rates and decreased by 61 % and 81 %, respectively, from 1990 to 2020. In contrast, the forest land and urban residential land is on an upward trend, with urban residential land showing the most significant expansion trend among all land use types.

From 1990 to 2020, the land use changes in the Heihe watershed were generally characterized as extensive urban expansion in the downstream Zhouzhi County, which led to the conversion of grassland and arable land to urban residential land. As a result, urban residential land expanded by nearly 22 km^2. In 2020, the urban residential land area was nearly twice than that in 1990. In the mountainous areas of the upstream water source, ecological conservation and returning farmland to forest projects contributed to the conversion of shrubland, grassland, and arable land to forest land, thus causing an increase in forest land area by approximately 90 km^2.

To comprehensively understand the intrinsic transformation relationships between various land use types, spatial data from the years 1990, 2000, 2010, and 2020 were analyzed. The results were analyzed to produce a land-use transfer matrix (Table 4) and a land-use transfer map (Fig. 7) for the study area, representing three different time periods. Combining the results from Table 4 and Fig. 6, it was observed that from 1990 to 2000, significant conversions from shrubland, grassland, and water bodies to arable land and urban residential land led to slight increase in the areas of the latter two categories. From 2000 to 2010, grassland was transformed into urban residential land, resulting in an expansion of urban residential land. Meanwhile, the completion of the Heihe Reservoir and other water conservancy facilities in 2002 expanded the area of water bodies. During the period from 2010 to 2020, urban residential areas expanded significantly, primarily by transforming grasslands and arable lands into residential area.

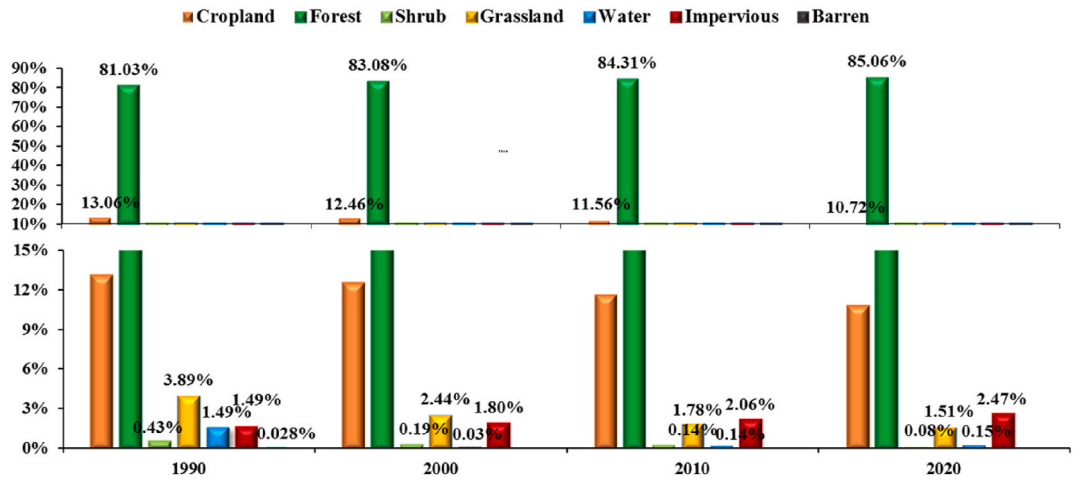

Fig. 6. Proportional area chart of land use types.

Table 4
Land use transition matrix of the Heihe watershed from 1990 to 2020 (unit: hm^2).

Period (years)	Type of land use	Arable land	Forest land	Shrubland	Grassland	Water bodies	Urban residential land
1990–2000	Arable land	26684.55	1171.62	7.38	426.78	1.89	604.17
	Forest land	268.83	178915.59	82.35	12.24	0	6.66
	Shrubland	51.48	527.13	221.13	149.67	0	0
	Grassland	470.25	3204	108	4810.95	1.89	16.74
	Water bodies	99.36	3.06	0	1.35	47.34	19.71
	Urban residential land	3.69	0	0	0	8.91	3273.3
	Unused land	1.8	0	0	0	0	59.76
2000–2010	Arable land	25031.25	1395	51.75	297.81	107.37	696.78
	Forest land	257.67	183505.14	39.33	16.74	0	2.52
	Shrubland	14.58	256.41	123.75	24.12	0	0
	Grassland	263.7	1395	101.25	3593.34	42.39	5.31
	Water bodies	6.3	0	0	0	46.35	7.38
	Urban residential land	7.47	0.45	0	0	117.72	3854.7
2010–2020	Arable land	22870.71	1544.49	8.01	175.32	16.56	965.88
	Forest land	432.81	186074.91	40.05	3.15	0	1.08
	Shrubland	45.72	116.91	115.92	37.53	0	0
	Grassland	307.08	467.73	19.53	3127.23	7.47	2.97
	Water bodies	46.98	5.49	0	1.26	235.89	24.21
	Urban residential land	16.83	0	0	0	80.46	4469.4

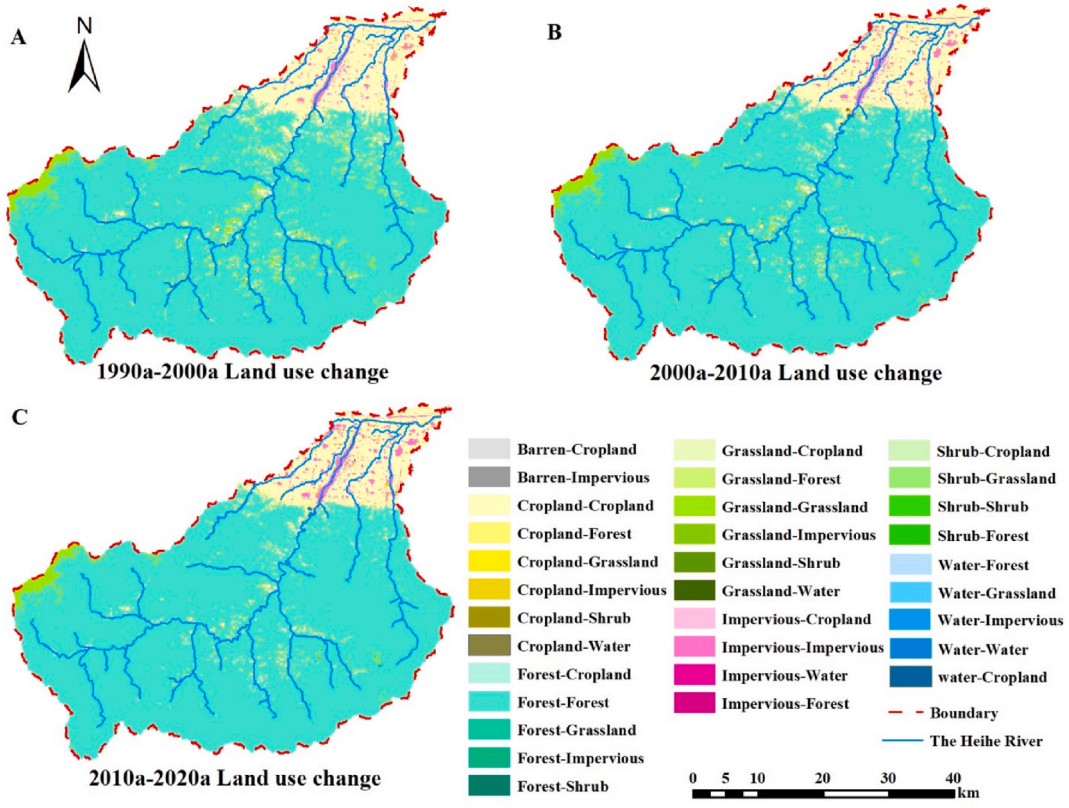

Fig. 7. Land use conversion map from 1990 to 2020.

4.2. Spatiotemporal analysis of PNPS risks

Using 1990 as the base year, the PNPI indicators for the study area were evaluated for each period using the quantile classification method. These indicators were classified into five distinct risk levels: very low, low, moderate, high, and very high (Fig. 8). The results indicate that from 1990 to 2020, significant changes occurred in areas with different levels of PNPS risk in the study area. The high and very-high risk areas in the urbanized regions downstream expanded during this period. The regions of PNPS risk within the study area have been summarized based on spatial change statistics (Fig. 9). The results show that from 1990 to 2020, the low-risk region

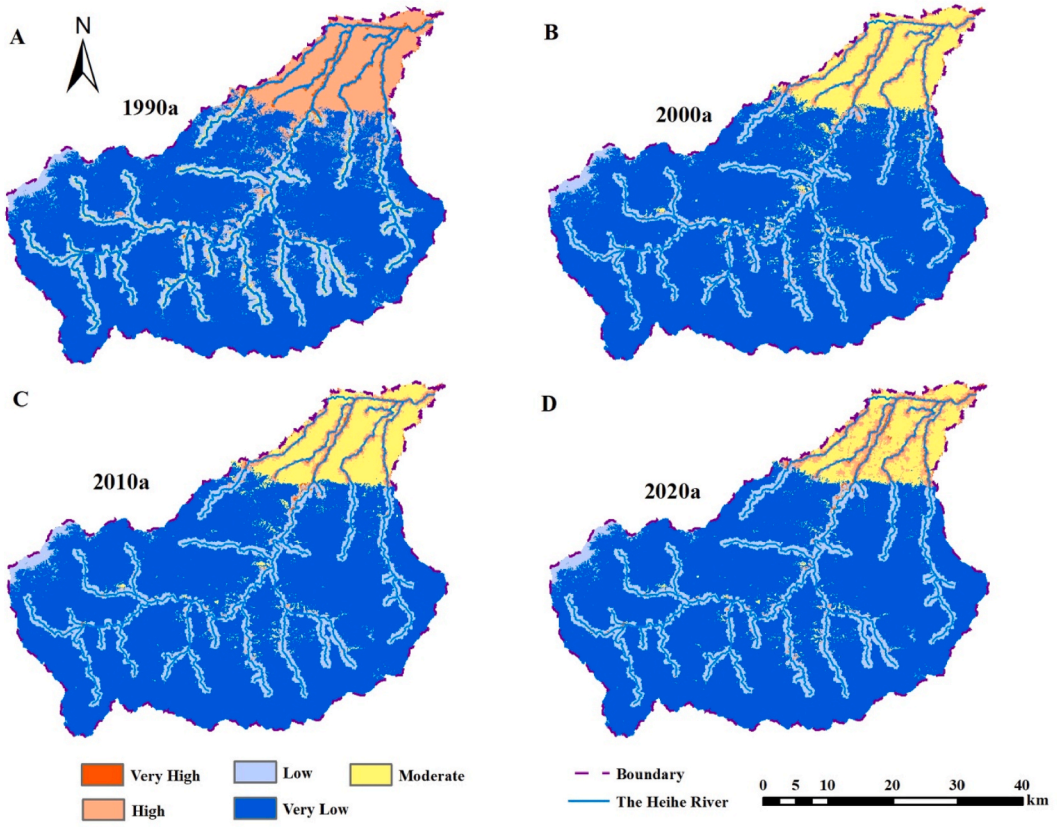

Fig. 8. Zoning map of PNPS risk for representative years.

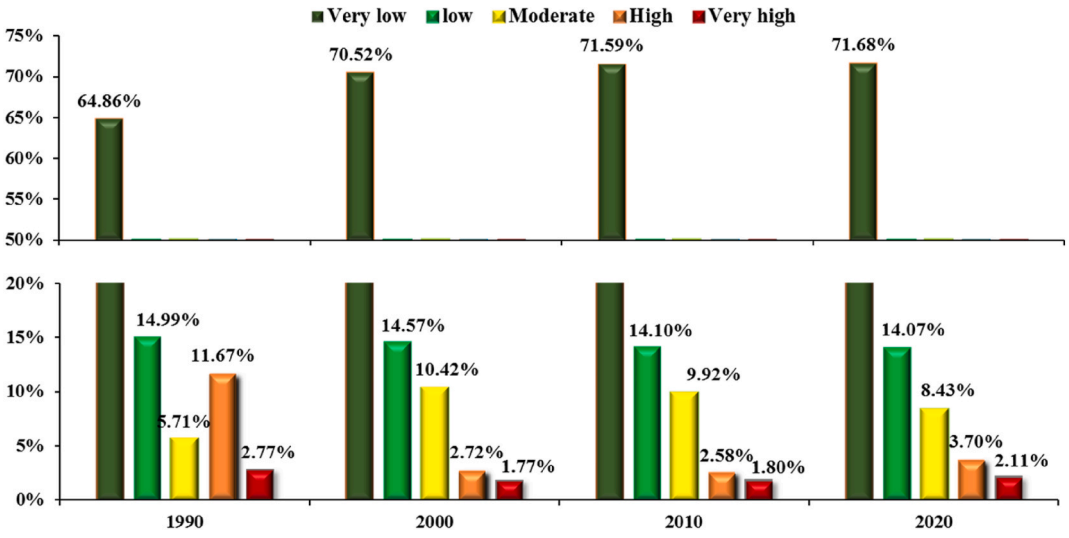

Fig. 9. Proportion map of regions with different levels of PNPS risk.

remained stable; the very low-risk region increased annually; the moderate-risk region reached a peak of 10 % in 2000 and gradually decreased thereafter; the high-risk region decreased by nearly 9 % from 1990 to 2000 and then showed an overall increasing trend; and the very high-risk region decreased by 1 % from 1990 to 2000 and increased annually thereafter.

To precisely capture the intrinsic transformation relationships among regions with varying risk levels, spatial data analysis was conducted on the zoning data of PNPS for 1990, 2000, 2010, and 2020 (Fig. 10), yielding a transition matrix of PNPS risks (Table 5) for

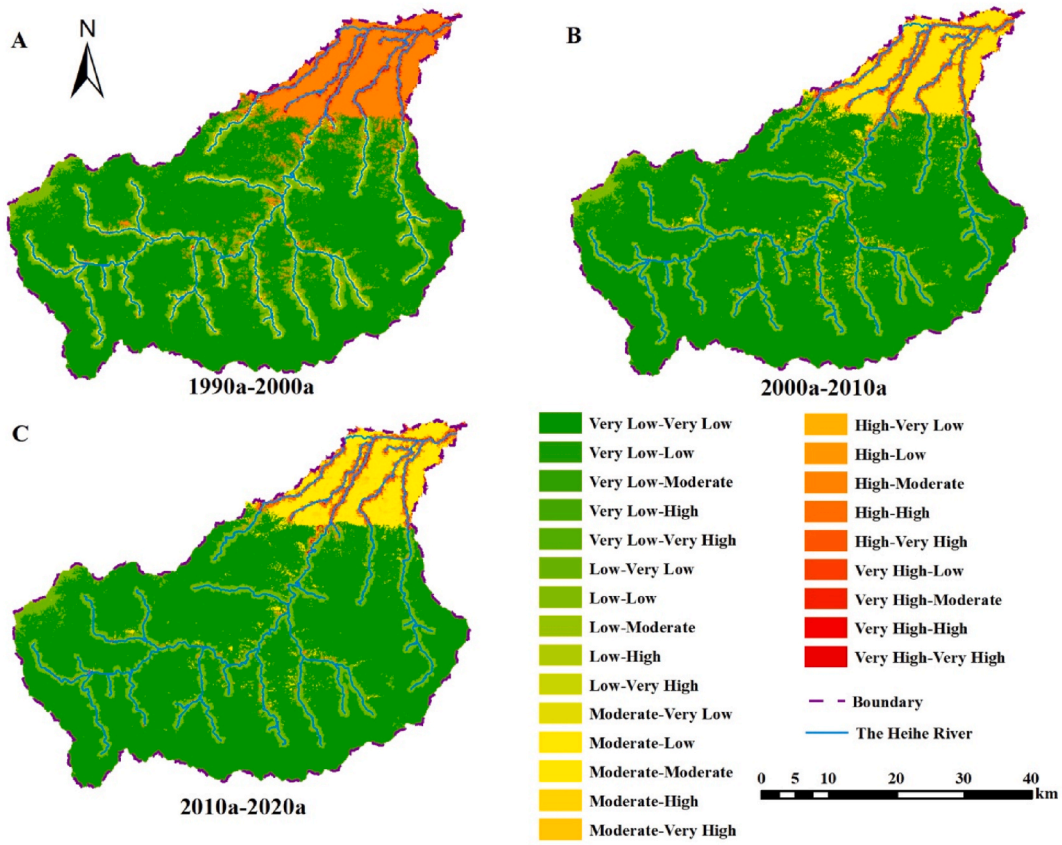

Fig. 10. Transition trend chart of regions with different levels of PNPS risk from 1990 to 2020.

Table 5
Transition matrix of PNPS risk in the Heihe watershed from 1990 to 2020 (unit: hm^2).

Period (years)	Risk level	Very low	Low	Moderate	High	Very high
1990–2000	Very low	143306.73	94.77	173.79	5.49	0.18
	Low	12006.36	20649.24	305.91	138.87	90.36
	Moderate	6.66	10761.3	1656.18	92.34	130.32
	High	804.51	468.09	20812.59	3708.99	42.03
	Very high	0	281.7	109.53	2074.95	3666.51
2000–2010	Very low	155705.58	291.24	113.49	12.87	1.08
	Low	1727.73	30063.15	262.98	98.82	102.42
	Moderate	977.04	280.17	21446.91	249.93	103.95
	High	86.58	330.84	86.49	5328.36	188.37
	Very high	0	261.09	41.58	31.23	3595.5
2010–2020	Very low	157207.32	1063.71	174.87	51.03	0
	Low	382.32	29420.64	1049.76	166.41	207.36
	Moderate	1027.17	167.04	17390.97	3255.84	110.43
	High	75.42	310.59	0.72	4685.85	648.63
	Very high	0	195.93	52.29	36.63	3706.47

the three study periods. The findings indicate that between 1990 and 2000, there was a notable change from high-risk to moderate-risk regions, leading to an expansion in the moderate-risk areas and a reduction in very high-risk areas. In contrast, the period from 2000 to 2010 saw relatively minor changes in the areas corresponding to each risk level. From 2010 to 2020, the high and very high-risk regions increased, mainly due to the conversion from the moderate-risk region to high and very high-risk regions.

Overall, high and very high-risk regions have been long concentrated in the middle and lower reaches. From 1990 to 2020, the PNPS risks in the Heihe watershed showed a polarized trend, with the moderate-risk region in urban residential areas, where human activities were concentrated, transforming into a high-risk region and the very high-risk region of arable land along the middle and lower reaches of the Heihe River expanding radially. The proportion of regions at or above the high-risk level increased from 4.49 % in 2000 to 5.81 % in 2020, representing a 29 % increase. The increment was attributed to the conversion of a large area of the moderate-

risk region. Meanwhile, the upstream water protection area saw a reduction in NPS risk.

4.3. Variation analysis of PNPS risks

An analysis of the spatiotemporal evolution characteristics of comprehensive land use and PNPS risks reveals a high degree of consistency in their spatial and temporal variation characteristics. Regions of high and very high risk have long been concentrated in urban residential land and arable land in the lower reaches of the Heihe River. The high-risk region decreased significantly by nearly 9 % from 1990 to 2000 and showed an overall increasing trend thereafter. In contrast, the very high-risk region shrank by 1 % from 1990 to 2000 and then increased annually. The primary land use types in areas with high or very high risks from 1990 to 2000 were arable land and urban residential land. Due to the relatively low level of urbanization in the lower reaches of the catchment in this period, the impact of urbanization on NPS risks was relatively small. Therefore, the main risk factors on arable land were related to crop planting. Before 1990, the main crops grown in the region were wheat, corn, melons, and fruits. Later, kiwi fruit became the main crop in the middle and lower reaches of the Heihe River. This has significantly reduced both the use of pesticides and fertilizers, resulting in a notable decline in the extent of high and very high-risk NPS regions in the downstream sections of the Heihe watershed during that period.

After 2000, the area of arable land used for the cultivation of kiwi fruit stabilized; therefore, the region of NPS risk affected by crop planting on arable land also stabilized. Meanwhile, urbanization accelerated, and the Heihe Reservoir was constructed, with resettlement projects being initiated in the reservoir area. Against this backdrop, the economy of downstream regions improved and the towns along the middle and lower reaches of the Heihe River expanded rapidly. As a result, the regions with very high PNPS risks expanded outward from these towns, making urban expansion the main driving factor for the variation in very high PNPS risk. In addition, after the official establishment of the Heihe Jinpen Reservoir water source area in 2002, a water source protection area of 1481 km^2 was delineated and water source protection measures, such as ecological migration and restoring agricultural land forest, were implemented. In the upstream region of the Heihe watershed, within the Qinling Mountain area, shrubland, grassland, and arable land were transformed into forest land. Consequently, the forested area expanded annually, resulting in a decrease in PNPS risk in the upper watershed.

According to an environmental quality report for Xi'an City, two water quality monitoring sections have been set up for the Heihe River: the Heihe Reservoir and the confluence of the Heihe and Weihe rivers. At the confluence, the water quality from 2001 to 2014 ranged from inferior Class V to Class IV. The main pollutants were petroleum, volatile phenols, and permanganate index. From 2015 to 2020, the water quality was good, ranging from Class III to Class II. From 2016 through 2020, the levels of ammonia nitrogen were observed to varied between 0.188 and 0.365 mg/L, and the total phosphorus concentrations varied between 0.02 and 0.05 mg/L. From 2011 to 2021, the water quality at the Heihe Reservoir water source monitoring point ranged from Class III to Class II. Based on the water quality conditions, four nutrient indicators, i.e., permanganate index, total nitrogen, ammonia nitrogen, and total phosphorus, were selected for analysis. Total nitrogen was the main indicator exceeding Class II water quality standards, total phosphorus remained relatively stable, and the other indicators showed an annual increasing trend. Among the water quality indicators, the permanganate index of the Heihe River ranged from 1.1 mg/L to 3.2 mg/L, ammonia nitrogen ranged from 0.146 mg/L to 0.243 mg/L, total nitrogen ranged from 0.85 mg/L to 2.30 mg/L, and total phosphorus ranged from 0.015 mg/L to 0.04 mg/L. Overall, the first three indicators showed an annual increasing trend, while total phosphorus remained relatively stable.

According to the monitoring results at the confluence of the rivers, water quality has improved significantly since 2015, reaching between Class III and Class II and meeting the requirements for Class III water bodies. This improvement is closely related to a series of point source treatment and ecological restoration measures taken by the government in recent years, such as the *Three-Year Action Plan of Xi'an City for Consolidating and Improving the Prevention and Control of Weihe River Water Pollution* implemented in 2012 and the *Implementation Plan of Xi'an City for the Treatment of Urban Black and Odorous Water Bodies* enacted starting in December 2018. These measures have enhanced water environmental management by means of rain and sewage diversion, municipal pipeline construction, sewage treatment capacity improvement, and river ecological restoration. However, according to the observations at the Heihe Reservoir, total nitrogen exceeded the standard and surpassed the Class II water quality standard for drinking water sources. The main reasons for the excess total nitrogen are the annual accumulation of soil erosion and the impact of living and production activities in the upstream protection area. In recent years, although soil and water conservation measures such as converting farmland to forests and grasslands have been implemented [40–42], the overall soil erosion in the watershed has been increasing annually. Therefore, managing NPS continues to be a crucial and difficult component of pollution prevention efforts in the study area.

5. Discussion

(1) Between 1990 and 2020, forest land and arable land were the predominant land use types in the Heihe watershed and consistently comprising around 95 % of the total land area, while shrubland, grassland, and unused land showed a decreasing trend. Specifically, grassland and shrubland shrank faster than other land use types over time, with the area decreasing by 61 % and 81 %, respectively. In contrast, forest land and urban residential land exhibited an increasing trend, with urban residential land exhibiting the fastest expansion rate. Moreover, the area of urban residential land in 2020 was nearly double that of 1990.

(2) Moderate and high-risk regions of NPS were mainly located in the middle and lower sections of the catchment. The area of the moderate risk reached a peak of 10 % in 2000 and then gradually decreased. The high-risk region decreased by nearly 9 % from 1990 to 2000 but showed an overall increasing trend thereafter. The very high-risk region shrank by 1 % from 1990 to 2000 but showed a yearly increasing trend thereafter. The high and very high-risk regions have long been concentrated in the middle and

lower riverbanks. The urban residential area, previously classified as a moderate-risk region due to concentrated human activities, transitioned into a high-risk zone, while the very high-risk region of arable land along the middle and lower stretches of the Heihe River expanded radially. The proportion of regions at or above the high-risk level increased from 4.49 % in 2000 to 5.81 % in 2020, representing a 29 % increase. The increment was attributed to the conversion of large areas of the moderate-risk region.

(3) The Heihe Jinpen Reservoir, located in the upper riverbank of the Heihe catchment area, was officially commissioned in 2002, thus establishing a 1481 km^2 water source protection area (Fig. 1). Moreover, measures such as ecological protection and conservation, returning farmland to forests, ecological migration, and point source control were implemented in the mountainous areas of the upstream water source. As a result, shrubland, grassland, and arable land were converted to forest land, causing forest land area to increase by approximately 90 km^2. This lowered the NPS risks in the upstream water source protection area. From 2011 to 2021, the water quality in Heihe Reservoir ranged between Class II and Class III, and the overall water quality was good. Total nitrogen was the main pollutant exceeding Class II standards, while total phosphorus remained relatively stable. The permanganate index and ammonia nitrogen levels showed a year-on-year increasing trend. The main reasons for the excess total nitrogen were the annual accumulation of soil erosion and the impact of living and production activities in the upstream protection area. This reflects that, although strict protection measures have been taken in water resource protection zones, the overall soil erosion in the watershed continues to worsen year by year. Soil erosion is related to natural and anthropogenic factors, making it a challenging aspect of NPS control.

(4) According to a combination of the spatial distribution and spatiotemporal evolution characteristics of the moderate and high-risk regions within the watershed with the actual water quality monitoring results, the following management measures have been proposed for the upstream water source area and the middle and lower riverbanks to facilitate the application of the research findings and provide technical support for government decision-making. The middle and lower riverbanks of the catchment are concentrated areas of moderate and high NPS risks. Therefore, effectively managing NPS requires focusing on the control of agricultural NPS. There are large area of arable lands and many moderate to high-risk regions downstream. In particular, most areas near the riverbanks are classified as high-risk regions. Therefore, it is essential to enhance the management of agricultural NPS by minimizing fertilizer and pesticide usage in farming and encouraging sustainable agricultural practices. Second, river ecological restoration must be performed. Vegetation should be planted on both sides of the river to reduce the direct entry of sediment and pollutants into the water. Third, pollutant emissions from daily production and living activities must be controlled. Residential land accounts for a high proportion in the lower reaches. The pollutants emitted from daily production and living activities will remain a key focus of water pollution control for some time. For uncollected and untreated non-point source wastewater, especially in rural areas, decentralized and centralized treatment measures should be adopted based on the actual situation to ensure compliance before discharge, which will decrease the discharge of untreated household wastewater into water bodies.

6. Conclusion

This study performed a case study on the Heihe watershed in the Qinling Mountains, a high ecologically sensitive area strongly influenced by human activities. By utilizing an enhanced PNPI model, the research examined the spatiotemporal variations and key factors influencing PNPS risks during the past 30 years, considering urban riverine land use changes within semi-arid areas. The primary conclusions are as follows.

(1) Arable land and forest land were the main types of land use in the Heihe watershed, primarily located in the lower and upper reaches, respectively. These two types of land accounted for approximately 95 % of the watershed area. From 1990 to 2020, the area of urban residential land surged, particularly around population centers like Zhouzhi County, in the lower reaches of the Heihe River. The area of urban residential land in the study region increased nearly 22 km^2. In 2020, the urban residential land area was nearly twice that in 1990, and it encroached upon a considerable area of grassland and arable land. In the upper river stream source protection area of the Qinling Mountains, there was an annual increase in the areas of shrubland, grassland, and arable land converted to forest land. As a result, the forest land area grew by approximately 90 km^2 over the 30-year period.

(2) The PNPS risks in the Heihe watershed showed a clearly polarized trend from 1990 to 2020. The region of high risk, mainly located in the arable land along the middle and lower reaches of the Heihe River, which is strongly affected by human activities, expanded radially. The proportion of high and very high-risk regions increased from 4.49 % in 2000 to 5.81 % in 2020, indicating that their proportion of area grew by 29 %. By contrast, the risk of NPS decreased within the upper river stream water source protection area in the Qinling Mountains.

(3) High consistency was observed between land use changes and spatiotemporal variations of PNPS risk. Regions with high and very high risk were primarily found in urban residential areas in the middle and lower riverbanks, as well as in cultivated lands along riverbanks. In contrast, areas with low and very low risk were predominantly situated in forest lands within the upstream Qinling Mountains. The expansion of urban residential land primarily contributed to high-risk regions increased in the watershed, while the expansion of forest land is the main factor for the rise of low and very low-risk regions.

(4) From 1990 to 2020, the Heihe watershed experienced significant land use changes driven by urbanization and ecological conservation measures. The risk posed by PNPS to the downstream environment continues to grow annually. The urban residential land and arable land along the riverbanks in the downstream area should be prioritized for NPS control or comprehensive watershed management in the future. To reduce pollution risks, measures such as controlling agricultural NPS and

restoring river ecology are suggested. In contrast, in the upper river stream water source area, measures such as ecological migration, conservation of water conservation forests, and soil erosion control are needed to reduce the NPS risks.

(5) The improved PNPI model was used to quantitatively analyze the spatial and temporal evolutionary characteristics of land use change on PNPS risk in the Heihe catchment and to examine factors underlying risk variations and water quality changes. The results of the quantitative analysis largely reflect the actual trends of factors influencing NPS in the watershed. This research has a significant reference value for controlling NPS and protecting water sources in other watersheds, especially in the Qinling Mountains. It also provides a technical basis and new ideas for scientific decision-making by government departments on NPS control within watersheds. The improved PNPI model is simple to operate, requires minimal data, and offers high accuracy. It has been applied in many watersheds and is highly applicable to the Heihe watershed. Nevertheless, certain empirical parameters within the model lack universal applicability due to differences in geographical environment and land use practices in different regions. In addition, the weight indicators depend on the weighting method, which may affect the results. Therefore, future research should compare different weighting and parameter selection methods to better mirror the actual non-point source risks in the study area.

Funding

This research was funded by the Scientific Innovation Practice Project of Postgraduates of Chang'an University (300103724020) and the Shaanxi Provincial Department of Education Serving the Special Project of Local Enterprises (23JE007).

Data availability Statement

The data that support the findings of this study are available from the corresponding author, Xiaolan Meng, upon reasonable request.

CRediT authorship contribution statement

Xiaolan Meng: Writing – original draft, Formal analysis, Conceptualization. **Fujun Xu:** Methodology, Investigation, Data curation. **Yuanjia Huang:** Resources, Methodology. **Xing Zhang:** Supervision, Software. **Mantong Zhang:** Writing – review & editing.

Declaration of competing interest

The authors declare that they have no known competing financial interests or personal relationships that could have appeared to influence the work reported in this paper.

References

[1] X. Yang, Q. Liu, X. Luo, et al., Spatial regression and prediction of water quality in a watershed with complex pollution sources, Sci. Rep. 7 (1) (2017) 8318.
[2] W. Ouyang, Y. Liu, S. Leng, et al., An analysis of research trends about non-point source pollution over the last three decades, Journal of Agro-Environment Science 37 (2018) 2234–2241.
[3] C.J. Vörösmarty, P.B. Mcintyre, M.O. Gessner, et al., Global threats to human water security and river biodiversity, Nature 467 (7315) (2010) 555–561.
[4] C. Puccinelli, S. Marcheggiani, M. Munafò, et al., Evaluation of aquatic ecosystem health using the potential non-point pollution index (PNPI) tool, Diversity of Ecosystems (2013), https://doi.org/10.5772/36330.
[5] F. Yang, Z. Xu, Y. Zhu, et al., Evaluation of agricultural nonpoint source pollution potential risk over China with a Transformed Agricultural Nonpoint Pollution Potential Index method, Environ. Technol. 34 (21–24) (2013) 2951–2963, https://doi.org/10.1080/09593330.2013.796008.
[6] H. Mohammadi, Hydrological Analysis of Flood Forecastin: Kasilaian Watershed, University of Mazandaran), 2001.
[7] Z. Gemesi, J.A. Downing, R.M. Cruse, et al., Effects of watershed configuration and composition on downstream lake water quality, J. Environ. Qual. 40 (2) (2011) 517–527, https://doi.org/10.2134/jeq2010.0133.
[8] J.H. Abdulkareem, W.N.A. Sulaiman, B. Pradhane, et al., Long-term hydrologic impact assessment of non-point source pollution measured through land use/land cover (LULC) changes in a tropical complex catchment, Earth Systems and Environment 2 (2018) 67–84, https://doi.org/10.1007/s41748-018-0042-1.
[9] X. Zhang, L. Zhou, Y.Q. Liu, Modeling land use changes and their impacts on non-point source pollution in a Southeast China coastal watershed, Int. J. Environ. Res. Publ. Health 15 (2018) 1593, https://doi.org/10.3390/ijerph15081593.
[10] J. Yang, J.P. Liang, G.H. Yang, et al., Characteristics of non-point source pollution under different land use types, Sustainability 12 (2020) 2012, https://doi.org/10.3390/su12052012.
[11] M. Munafò, G. Cecchi, F. Baiocco, et al., River pollution from non-point sources: a new simplified method of assessment, J. Environ. Manag. 77 (2) (2005) 93–98, https://doi.org/10.1016/j.jenvman.2005.02.016.
[12] M. Cotman, A. Drolc, J.Z. Koncan, Assessment of pollution loads from point and diffuse sources in small river basin: case study Ljubljanica river, Environ. Forensics 9 (2–3) (2008) 246–251, https://doi.org/10.1080/15275920802122965.
[13] H. Zhang, G.H. Huang, Assessment of non-point source pollution using a spatial multicriteria analysis approach, Ecol. Model. 222 (2) (2011) 313–321, https://doi.org/10.1016/j.ecolmodel.2009.12.011.
[14] R. Geng, M. Li, X. Wang, et al., Effect of land use/landscape changes on diffuse pollution load from watershed based on swat model, Trans. Chin. Soc. Agric. Eng. 31 (16) (2015) 241–250, https://doi.org/10.11975/j.issn.1002-6819.2015.16.032.
[15] A.O. Alnahit, A.K. Mishra, A.A. Khan, Quantifying climate, streamflow, and watershed control on water quality across Southeastern US watersheds, Sci. Total Environ. 739 (2020) 139945, https://doi.org/10.1016/j.scitotenv.2020.139945.
[16] B. Gossweiler, I. Wesström, I. Messing, et al., Impact of land use change on non-point source pollution in a semi-arid catchment under rapid urbanisation in Bolivia, Water 13 (2021) 410, https://doi.org/10.3390/w13040410.
[17] E. Contreras, C. Aguilar, M.J. Polo, Accounting for the annual variability when assessing non-point source pollution potential in Mediterranean regulated watersheds, Sci. Total Environ. 902 (2023) 167261, https://doi.org/10.1016/j.scitotenv.2023.167261.

[18] J. Lyu, Y. Huang, Q. Nie, et al., Spatiotemporal variations and risk characteristics of PNP driven by LUCC in the Loess Plateau Region, China, Frontiers in Ecology and Evolution 11 (2023) 1253328, https://doi.org/10.3389/fevo.2023.1253328.
[19] W. Ouyang, A.K. Skidmore, A.G. Toxopeus, et al., Long-term vegetation landscape pattern with non-point source nutrient pollution in upper stream of Yellow River basin, J. Hydrol. 389 (3–4) (2010) 373–380, https://doi.org/10.1016/j.jhydrol.2010.06.020.
[20] D.K. Borah, M. Bera, Watershed-scale hydrologic and nonpoint-source pollution models: review of applications, Transactions of the ASAE. American Society of Agricultural Engineers 47 (3) (2004) 1553566, https://doi.org/10.13031/2013.16110.
[21] A. Sharma, K.N. Tiwari, Predicting non-point source of pollution in maithon reservoir using a semi-distributed hydrological model, Environ. Monit. Assess. 191 (8) (2019) 522, https://doi.org/10.1007/s10661-019-7674-y.
[22] L. Hou, Z. Zhou, R. Wang, et al., Research on the nonPoint source pollution characteristics of important drinking water sources, Water 14 (2022) 211, https://doi.org/10.3390/w14020211.
[23] G. Hao, J. Li, H. Li, et al., Advances in research of watershed non-point source pollution models and uncertainty analysis methods, J. Hydroelectr. Eng. 37 (2018) 54–64, https://doi.org/10.11660/slfdxb.20181206.
[24] G. Cecchi, M. Munafò, F. Baiocco, et al., Estimating river pollution from diffuse sources in the Viterbo province using the potential non-point pollution index, Annali dell'Istituto superiore di sanità 43 (3) (2007) 295–301.
[25] Z.Y. Shen, X.S. Hou, W. Li, et al., Relating landscape characteristics to non-point source pollution in a typical urbanized watershed in the municipality of Beijing, Landsc. Urban Plann. 123 (2014) 96–107, https://doi.org/10.1016/j.landurbplan.2013.12.007.
[26] K. Loague, D.L. Corwin, Uncertainty in regional-scale assessments of non-point source pollutants, in: D.L. Corwin, K. Loague (Eds.), Applications of GIS to the Modeling of Non-Point Source Pollutants in the Vadose Zone, Soil Science Society of America), Madison, 1996, pp. 131–152.
[27] Y. Liu, C. Yang, X. Yu, et al., Monitoring the landscape pattern and characteristics of non-point source pollution in a mountainous river basin, Int. J. Environ. Res. Publ. Health 18 (21) (2021) 11032, https://doi.org/10.3390/ijerph182111032.
[28] Y. Qian, L. Sun, D. Chen, et al., The response of the migration of non-point source pollution to land use change in a typical small watershed in a semi-urbanized area, Sci. Total Environ. 785 (2021) 147387, https://doi.org/10.1016/j.scitotenv.2021.147387.
[29] H. Li, J. Zhang, S. Zhang, et al., A framework to assess spatio-temporal variations of PNP risk for future land-use planning, Ecol. Indicat. 137 (2022) 108751, https://doi.org/10.1016/j.ecolind.2022.108751.
[30] G. Cecchi, L. Mancini, M. Munafò, et al., Assessment of Potential River Pollution from Non-point Sources in the Viterbo Province, Academic Press, 1982.
[31] T. Li, X. Wu, Study on the potential pollution in river section based on PPI, Environ. Sci. J. Integr. Environ. Res. 31 (2010) 2619–2626.
[32] D. Shi, S. Zhang, H. Wang, Risk analysis of spatiotemporal variation of PNP in the upper reaches of the Beisha River, Research of Environmental Science 33 (2020) 921–931.
[33] Q. Nie, J. Lv, X. Sun, et al., Spatial and temporal variations of non-point source pollution risk affected by land use changes in Bahe River Basin, Journal of Water Resources and Water Engineering 30 (2019) 80–88.
[34] Y.P. Fan, C.L. Fang, A comprehensive insight into water pollution and driving forces in Western China—case study of Qinghai, J. Clean. Prod. 274 (2020) 123950, https://doi.org/10.1016/j.jclepro.2020.123950.
[35] H.L. Li, J.J. Zhang, Y.F. Zhang, et al., Analysis of spatial-temporal variation characteristics of PNP risks in the upper beiyun river basin using different weighting methods, Huanjing Kexue 42 (6) (2021) 2796–2809, https://doi.org/10.13227/j.hjkx.202010225.
[36] D. Ierodiaconou, L. Laurenson, M. Leblanc, et al., The consequences of land use change on nutrient exports: a regional scale assessment in south-west Victoria, Australia, J. Environ. Manag. 74 (4) (2005) 305–316, https://doi.org/10.1016/j.jenvman.2004.09.010.
[37] F. Clement, J. Ruiz, M.A. Rodrıguez, et al., Landscape diversity and forest edge density regulate stream water quality in agricultural catchments, Ecol. Indicat. 72 (2017) 627–639, https://doi.org/10.1016/j.ecolind.2016.09.001.
[38] K. Zhao, J. Li, X. Ma, et al., The effects of land-use and climatic changes on the hydrological environment in the Qinling Mountains of Shaanxi Province, Forests 13 (2022) 1776, https://doi.org/10.3390/f13111776.
[39] G.Y. Cui, Y. Zhang, Y. Chao, et al., Land use change and eco-environmental effects in Qinling Mountains in Recent 40Years, Res. Soil Water Conserv. 30 (1) (2023) 319–326, https://doi.org/10.13869/j.cnki.rswc.20220301.002.
[40] Y. Xu, H. Li, H. Jia, Estimate the loss load of non-point source pollution by soil and water loss in Heihe Basin of Shaanxi Province, Bull. Soil Water Conserv. 25 (2005) 78–80.
[41] D. Zhu, Study on the Pollution Source Situation and Protection for Urban Drinking Water Sources-The Heihe Jinpen Reservoir, Chang'an University, 2014.
[42] X. Wang, Source and Characterization of Dissolved Organic Matter (DOM) in Jinpen Reservoir, Xi'an University of Architecture and Technology, 2018, p. 6.
[43] X.J. Mao, T.L. Huang, N. Li, et al., Sources and distribution of phosphorus in sediments of the Jinpen Reservoir, Environ. Sci. J. Integr. Environ. Res. 40 (2019) 2739–2744.
[44] Z. Shen, L. Chen, X. Ding, et al., Long-term variation, (1960–2003) and causal factors of non-point-source nitrogen and phosphorus in the upper reach of the Yangtze River, J. Hazard Mater. 252–253 (2013) 45–56, https://doi.org/10.1016/jjhazmat.2013.02.039.
[45] Y. Tao, J. Liu, X. Guan, et al., Estimation of potential agricultural non-point source pollution for Baiyangdian Basin, China, under different environment protection policies, PLoS One 15 (9) (2020) e0239006, https://doi.org/10.1371/journal.pone.0239006.